Tradeoffs in soil carbon protection mechanisms under aerobic and anaerobic conditions

Running head: Tradeoffs in anoxic C protection

Wenjuan Huang[1], Chenglong Ye[1,2], William Hockaday[3], Steven J. Hall[1*]

[1]Department of Ecology, Evolution, and Organismal Biology, Iowa State University, Ames, IA 50011, USA

[2]Ecosystem Ecology Lab, College of Resources and Environmental Sciences, Nanjing Agricultural University, Nanjing 210095, China

[3]Department of Geosciences, Baylor University, Waco, TX 76798, USA

*Corresponding author

Email: stevenjh@iastate.edu; Phone: 515-294-7650; Fax: 515-294-1337

This article has been accepted for publication and undergone full peer review but has not been through the copyediting, typesetting, pagination and proofreading process, which may lead to differences between this version and the Version of Record. Please cite this article as doi: 10.1111/GCB.15100

Abstract

Oxygen (O_2) limitation is generally understood to suppress soil carbon (C) decomposition and is a key mechanism impacting terrestrial C stocks under global change. Yet, O_2 limitation may differentially impact kinetic or thermodynamic vs. physico-chemical C protection mechanisms, challenging our understanding of how soil C may respond to climate-mediated changes in O_2 dynamics. Although O_2 limitation may suppress decomposition of new litter C inputs, release of physico-chemically protected C due to iron (Fe) reduction could potentially sustain soil C losses. To test this tradeoff, we incubated two disparate upland soils that experience periodic O_2 limitation—a tropical rainforest Oxisol and a temperate cropland Mollisol—with added litter under either aerobic (control) or anaerobic conditions for one year. Anoxia suppressed total C loss by 27% in the Oxisol and by 41% in the Mollisol relative to the control, mainly due to the decrease in litter-C decomposition. However, anoxia sustained or even increased decomposition of native soil-C (11.0% vs. 12.4% in the control for the Oxisol and 12.5% vs. 5.3% in the control for the Mollisol, in terms of initial soil C mass), and it stimulated losses of metal- or mineral-associated C. Solid-state ^{13}C nuclear magnetic resonance spectroscopy demonstrated that anaerobic conditions decreased protein-derived C but increased lignin- and carbohydrate-C relative to the control. Our results indicate a tradeoff between physico-chemical and kinetic/thermodynamic C protection mechanisms under anaerobic conditions, whereby decreased decomposition of litter C was compensated by more extensive loss of mineral-associated soil C in both soils. This challenges the common assumption that anoxia inherently protects soil C and illustrates the vulnerability of mineral-associated C under anaerobic events characteristic of a warmer and wetter future climate.

Keywords: Anaerobic; Anoxic; ^{13}C NMR; Carbon stable isotope; C3/C4 plant; DOC; Iron reduction; Litter decomposition; Mineral-associated carbon; Oxygen

Introduction

Oxygen (O_2) availability has been long known to impact soil organic matter (SOM) decomposition. The scarcity of O_2 often reduces carbon (C) mineralization rates as a consequence of kinetic and thermodynamic constraints on SOM depolymerization and microbial metabolism, which have been most commonly studied in wetlands and sediments (Arndt et al., 2013; Freeman et al., 2001; LaRowe & Van Cappellen, 2011; McLatchey & Reddy, 1998). However, many, if not most, upland soils contain anaerobic microsites resulting from biological O_2 demand that exceeds physical O_2 supply (Hall & Silver, 2015; Keiluweit et al., 2016; Sexstone et al., 1985; von Fischer & Hedin, 2007). Many upland soils can also experience periodic bulk (macropore-scale) O_2 limitation following periods of high precipitation or irrigation, snowmelt, and/or soil frost (Hall et al., 2016; Krichels et al., 2019; Moyes & Bowling, 2013; Silver et al., 1999). Anoxia is thus increasingly understood as a key mechanism contributing to SOM persistence in upland soils and at terrestrial-aquatic interfaces (Boye et al., 2017; Hall & Silver, 2015; Keiluweit et al., 2016, 2018). Furthermore, soil O_2 availability at the microsite and bulk scales may be strongly coupled to changes in the frequency and intensity of precipitation expected with global change, given the critical role of soil moisture in regulating gas diffusion (Liptzin, Silver, & Detto, 2011; O'Connell, Ruan, & Silver, 2018). However, quantifying the magnitude of the impacts of O_2 limitation on decomposition remains a critical knowledge gap for predicting C persistence in upland soils, especially in response to climate-mediated changes in soil O_2 availability.

In uplands, physico-chemical associations between SOM and minerals, including iron (Fe) (oxyhydr)oxides, are among the most important mechanisms contributing to soil C persistence (Kleber et al., 2015). However, organic C sorbed or co-precipitated with iron (Fe) oxides can be released under anaerobic conditions as a consequence of dissimilatory Fe reduction (Buettner et al., 2014; Hagedorn et al., 2000; Thompson et al., 2006) and thus become vulnerable to microbial decomposition. The release of Fe mineral-associated organic C under conditions of limited O_2 availability can stimulate C mineralization by facilitating microbial access to previously protected C (Huang & Hall, 2017b). This implies a potential trade-off in SOM protection mechanisms under

anaerobic vs. aerobic conditions: the kinetic/thermodynamic constraints imposed by O_2 limitation could coincide with partial loss of mineral protection. However, little is understood to what degree increased decomposition of released mineral-associated C might compensate for suppressed decomposition of other C sources under anaerobic conditions, especially due to the critical role of SOM biochemical composition in mediating that response.

Oxygen limitation is increasingly recognized to preferentially preserve reduced compounds (e.g., lipids) relative to oxidized ones (e.g., carbohydrate and proteins) due to thermodynamic constraints on microbial oxidation of reduced compounds (LaRowe & Van Cappellen, 2011). For example, a carbohydrate with a nominal oxidation state near zero can in principle be readily oxidized by a wide range of terminal electron acceptors, whereas a lipid with a nominal oxidation state of -2 cannot be oxidized by electron acceptors other than O_2, nitrate, or manganese oxide (Keiluweit et al., 2016). A separate kinetic constraint is likely to lead to accumulation of lignin and polyaromatics under anaerobic conditions (Freeman et al., 2001). This is because the initial depolymerization of these molecules is mediated by enzymes (peroxidases and oxidases) or reactive oxygen species which require a source of molecular O_2 or hydrogen peroxide for their activity (Kirk & Farrell, 1987). In contrast, the hydrolytic depolymerization of carbohydrates and proteins does not require the presence of O_2 and may be little affected by anoxia (Hall, Treffkorn, & Silver, 2014). Moreover, Fe reduction under anaerobic conditions more readily released non-aromatic compounds from mineral protection relative to aromatic C (Han et al., 2019; Mejia et al., 2018). Together, these findings suggest that even while anaerobic conditions could facilitate transient accumulation of highly reduced C (e.g., lipids) or hydrolysis-resistant C (e.g. lignin) due to O_2 limitation, the decomposition of relatively oxidized C substrates such as carbohydrates and proteins could increase following their release from physico-chemical protection.

Here we studied how anaerobic conditions affected the physico-chemical protection, molecular composition, and decomposition of C in two upland soils with greatly contrasting climate, geochemical, and biological attributes—an Oxisol from a humid tropical forest and a

Mollisol from a temperate cropland—to address the generality of potential tradeoffs in SOM protection and compositional shifts under aerobic (control) and anaerobic conditions. The soils were amended with C_4 grass litter, which enabled us to discriminate between two different C sources (new litter-C vs. extant soil-C) using stable isotope ratio ($\delta^{13}C$) measurements of C mineralization (CO_2 and CH_4 production) and chemically extractable C pools. Molecular C composition was characterized by solid-state ^{13}C nuclear magnetic resonance (NMR) spectroscopy at the beginning and end of the incubation. We hypothesized that (1) the decomposition of soil C would be suppressed less than the decomposition of litter C under anaerobic conditions; and (2) increased losses of relatively oxidized C compounds (e.g., carbohydrate and proteins) as compared with compounds that were relatively reduced (e.g., lipids) or resistant to hydrolysis (e.g. lignin) would sustain soil C decomposition under anaerobic conditions.

Materials and Methods

Sample preparation

We collected soil samples from an Oxisol in a humid tropical forest near the El Verde field station of the Luquillo Experimental Forest (18°17′N, 65°47′W), Puerto Rico and a Mollisol from a temperate cropland in north-central Iowa (41°75′N, 93°41′W), USA. Both soils experience periodic O_2 limitation and Fe reduction in microsites and bulk soil as a consequence of episodically high rainfall, high clay content, and low position in the landscape (Huang & Hall, 2017b; O'Connell et al., 2018). The surface A horizons from the Oxisol (0 – 10 cm) and Mollisol (0 – 20 cm) soils were collected and gently mixed. Soil organic C measured 44.8 mg C g^{-1} in the Oxisol and 35.1 mg C g^{-1} in the Mollisol, and the C:N ratio was 10.8 in the Oxisol and 11.3 in the Mollisol. More details on soil characteristics and sampling locations are provided in Table S1. Subsamples of field-moist soils (5 g dry mass equivalent) were gently homogenized with 0.5 g C_4 litter (ground leaf tissue of *Andropogon gerardii*, big bluestem) to provide an isotopic contrast between litter- and soil-C (the Oxisol had C_3 and the cropland had mixed C_3-C_4 vegetation history).

The $\delta^{13}C$ value of soil organic C was -28.4‰ for the Oxisol, -21.5‰ for the Mollisol and -11.3‰ for the C_4 litter. The C_4 litter had 38.2% C and 0.68% N (C:N ratio of 56).

Headspace treatments

Soils were incubated under static aerobic (control) or anaerobic treatments at field moisture capacity (1.01 g H_2O g^{-1} soil for the Oxisol and 0.46 g H_2O g^{-1} soil for the Mollisol) for 384 days in the dark at 23 °C (n = 5 per treatment). Samples were flushed with humidified CO_2-free air following each gas measurement to achieve aerobic conditions or with humidified dinitrogen for anaerobic conditions, and water was added as necessary to replace moisture lost during headspace flushing. Each replicate remained sealed in a gas-tight glass jar (946 mL) during the incubation.

Cumulative C mineralization

We measured total carbon dioxide (CO_2) and methane (CH_4) production and their $\delta^{13}C$ values with a tunable diode laser absorption spectrometer (TDLAS, TGA200A, Campbell Scientific, Logan, Utah, USA) (Hall et al., 2017; Huang & Hall, 2018) and gas chromatograph (GC-2014, Shimadzu, Columbia, MD) over 2–4 day intervals. Cumulative total mineralized C (CO_2 + CH_4) calculated after 384 days was partitioned into litter- and soil-derived C using a two-source mixing model (Huang & Hall, 2018) as discussed below. The cumulative $\delta^{13}C$ values of total mineralized C were calculated as a flux-weighted average of $\delta^{13}C$ values of CO_2 and CH_4. While the $\delta^{13}C$ values of CH_4 are systematically lower than the organic substrates from which it is derived, the $\delta^{13}C$ of CO_2 produced in methanogenic environments is correspondingly greater by mass balance (Huang & Hall, 2018). Therefore, given that kinetic isotope fractionation is minor or negligible during soil organic C decomposition (Breecker et al., 2015; Ehleringer et al., 2000; Hall et al., 2017), the mass-weighted $\delta^{13}C$ values of total mineralized C (CO_2 + CH_4) approximately reflect the $\delta^{13}C$ values of the decomposed organic substrates. Total organic C mineralization and its cumulative $\delta^{13}C$ values from the Mollisol were corrected for small losses of carbonate (0.58 mg C g^{-1} soil) as CO_2 (Huang & Hall, 2018). Briefly, carbonate C concentrations and their $\delta^{13}C$ values were measured at the beginning and the end of incubation using a method modified after Amundson et al. (1988). The $\delta^{13}C$ values of carbonate averaged -1.3‰ and did not change during the incubation.

A two-source mixing model was used to calculate the cumulative $\delta^{13}C$ value of total mineralized organic C, correcting for the small carbonate contribution (Huang & Hall, 2018).

The end-member $\delta^{13}C$ value of respired litter C (-11.4‰) was determined by a 32-day incubation of litter with a soil microbial inoculum under aerobic conditions (Supporting Information, Methods and Fig. S1). This value agreed closely with the predicted $\delta^{13}C$ values of litter carbohydrates, which are on average ~2‰ greater than bulk litter C (-13.3‰) (Bowling et al., 2008). This observation is further consistent with our NMR data (Table S2), which showed that carbohydrate was the dominant C source (72%) in the added litter C. Litter incubated under anaerobic conditions in the absence of soil decomposed very little, measuring only ~7% of C mineralization under aerobic conditions after 32 days, with CH_4 production near detection limit (~0.03% of total C mineralization). This was consistent with the importance of soil terminal electron acceptors (e.g., Fe and electron-accepting organic moieties) for sustaining anaerobic decomposition. Therefore, we used the same end-member value of litter C for both the aerobic and anaerobic treatments, given that our NMR data showed that carbohydrate was both the dominant source of litter C inputs (Table S2) and C loss (Table 1) in both treatments, and that unprotected carbohydrates can be decomposed using soil terminal electron acceptors (Keiluweit et al., 2016). To assess the influence of this end-member assumption, we conducted a sensitivity analysis where we increased or decreased the $\delta^{13}C$ value of the litter end member by 1‰ in the anaerobic treatments, consistent with possible relative shifts in the decomposition of compounds with relatively higher (carbohydrates, proteins) or lower (lipids, lignins) $\delta^{13}C$ values. Altering the litter end-member values did not qualitatively affect our conclusions (Table S3).

We used different end member values for soil organic C between the control and anaerobic treatment. The time-integrated $\delta^{13}C$ values of soil respired CO_2 in aerobic incubations are typically equivalent to those of bulk soil organic C in topsoils under aerobic conditions (Breecker et al., 2015; Hall et al., 2017). Therefore, we used the $\delta^{13}C$ value of soil organic C (-28.4‰ for the Oxisol and -21.5‰ for the Mollisol) as the proxy for respired soil C in the control. Because anaerobic conditions may inhibit decomposition of lignin and lipids (Gao et al., 2016), which have

lower $\delta^{13}C$ values than other organic molecules (Bowling et al., 2008) and are more significant components of soil organic C than litter (Table 1 and Table S2), we assessed the soil C end members by incubating litter-free soils under anaerobic conditions for 384 days (Supporting Information, Methods). The cumulative $\delta^{13}C$ value of total respired C after 384 days measured -26.6 ± 0.1‰ for the Oxisol and -18.3 ± 0.3‰ for the Mollisol (Fig. S2).

Soil biogeochemical analyses

To understand the mechanisms controlling decomposition of different C sources (soil vs. litter C) in response to O_2 limitation, we used chemical extractions to test how the anaerobic treatments affected Fe species and organic C associated with Fe. At the end of this experiment, subsamples of soils used in the incubations were measured for dissolved organic C (DOC) and metals in several extraction solutions, interpreted as follows: water-soluble C (DOC_{H_2O}); sodium sulfate (C from weak polyvalent cation bridges, $DOC_{Na_2SO_4}$); sodium dithionite (C sorbed to or co-precipitated with reducible Fe phases, $DOC_{Na_2S_2O_4}$); and sodium pyrophosphate (C in non-reducible organo-metal/mineral complexes, $DOC_{Na_4P_2O_7}$). For DOC_{H_2O}, soil subsamples (n = 5) were extracted by nanopure water in a 1:60 dry soil-to-solution ratio. For Fe oxyhydroxides and organic C in the additional soil extractions, which were conducted sequentially, soil subsamples (n = 5) were first extracted by 0.5 M sodium sulfate at a 1:180 dry soil-to-solution ratio for 1 h, and the residue was extracted with 0.05 M sodium dithionite at the same ratio for 16 h. After that, the residue was extracted with 0.05 M HCl for 1 h to re-dissolve any sulfide-precipitated Fe and then extracted with 0.1 M $Na_4P_2O_7$ for 16 h (Huang et al., 2019). The average pH in the sodium sulfate extraction was 5.36 for the Oxisol and 9.51 for the Mollisol, and pH in the sodium dithionite extraction was 4.91 for the Oxisol and 3.60 for the Mollisol. Differences in pH between soils reflected interactions between soil geochemical composition and the extractant solutions (i.e., differences in buffering capacity and formation of acidic products of dithionite oxidation, and dissolution of calcium carbonates in the Mollisol due to excess sodium). Although pH may

influence the absolute amount of C released in the two extractions between soils, the relative responses of DOC to headspace treatments within a soil type would not be affected. Concentrations of DOC in the sodium sulfate extractions were corrected for DOC measured in the above-mentioned separate water extraction. Iron concentrations in 0.05 M $Na_2S_2O_4$ and 0.05 M HCl were measured colorimetrically (Huang & Hall, 2017a), and Fe concentrations in 0.1 M $Na_4P_2O_7$ were analyzed by inductively coupled plasma optical emission spectrometry (ICP-OES; Perkin Elmer Optima 5300 DV, Waltham, Massachusetts).

To determine the drivers of C release under the anaerobic conditions, we measured Fe reduction and soil pH at the end of incubation. The concentrations of Fe(II) and Fe(III) were measured in 0.5M HCl extractions at a 1:60 dry soil-to-solution ratio (termed Fe_{HCl}, n = 5). The Fe(II) released in 0.5M HCl largely reflects soluble and exchangeable Fe^{2+}, and may also include contributions from Fe(II) phases such as siderite and magnetite (Chen et al., 2018). The 0.5M HCl extraction also solubilizes a highly reactive fraction of Fe(III)-bearing mineral phases which are smaller than the total short-range-ordered Fe pool (Hall & Silver, 2015). Soil subsamples (n = 3) were similarly extracted prior to the experiment in order to calculate net changes in Fe(II) (i.e., net Fe reduction). Concentrations of $Fe(II)_{HCl}$ and $Fe(III)_{HCl}$ were determined colorimetrically using an optimized ferrozine method (Huang & Hall, 2017a). Soil pH (n = 3) was measured in 1:2.5 slurries of soil and deionized water.

To examine the responses of different extracted C sources to anaerobic conditions, we used DOC concentrations and their $\delta^{13}C$ values to calculate the litter- and soil-derived DOC in each extraction by a two-source mixing model (Huang & Hall, 2017b). The DOC concentrations and their $\delta^{13}C$ values in the soil extractions were analyzed by measuring CO_2 concentrations and $\delta^{13}C$ of CO_2 produced from oxidation of total DOC by boiling with persulfate in serum vials followed by injection of the headspace gas to the TDLAS (Huang & Hall, 2017b; Lang et al., 2012). The end-member values used in the two-source mixing model were derived from $\delta^{13}C$ of the respective sources: -13.3‰ for litter, -28.4‰ for the Oxisol, and -21.5‰ for the Mollisol. To test the validity of these end members, we extracted DOC from the litter and soils alone prior to the experiment

using the methods described above. We found that the $\delta^{13}C$ values of DOC from the litter (-13.6 ± 0.2‰) and soils alone (Oxisol: -28.5 ± 1.2‰; Mollisol: -22.6 ± 1.5‰) were indistinguishable from their respective bulk C sources, justifying the use of these $\delta^{13}C$ values as end members in the mixing model. We acknowledge that C molecules contributing to SOM and DOC have differing $\delta^{13}C$ values (Bowling et al., 2008), and that $\delta^{13}C$ values of DOC may be subtly altered by isotopic fractionation during sorption and release from minerals (Kaiser et al., 2001). However, the $\delta^{13}C$ values of DOC extracted from the soils alone by Na_2SO_4 (Oxisol: -28.7 ± 0.3‰; Mollisol: -20.7 ± 0.9‰), dithionite (Oxisol: -27.5 ± 0.3‰; Mollisol: -22.0 ± 1.4‰) and pyrophosphate (Oxisol: -28.0 ± 0.2‰; Mollisol: -21.6 ± 0.2‰) were also similar to their respective $\delta^{13}C$ values of bulk soil C. This similarity indicated that the $\delta^{13}C$ values of DOC were not greatly affected by the compound-specific sorption of C released in these different chemical extraction solutions.

^{13}C nuclear magnetic resonance (NMR) spectroscopy. From each soil, three subsamples from the anaerobic treatment and two subsamples from the control were collected after the 384-day incubation and analyzed by ^{13}C NMR to assess organic C molecular composition (a technical error prevented analysis of the third control replicate). We also analyzed organic C molecular composition in additional soil samples combined with litter at the beginning of the incubation to calculate total mass loss of each C molecular component after the 384-day incubation. An additional sample of litter was analyzed without soil present. Soil was pre-treated with hydrochloric acid (HCl, 10%) and hydrofluoric acid (HF, 10%) to remove calcium carbonate and mineral phases, including paramagnetics, to increase the NMR sensitivity (Gélinas et al., 2001). Briefly, 2–3 g of finely-ground soil was shaken with 30 ml HCl (10% wt.) for 30 min, centrifuged and decanted. Soils were shaken with 40 mL of HF (10% wt.) and HCl (10% wt.) for 8 h and centrifuged. The supernatants were decanted, and this procedure was repeated for a total of four times. Each pellet was washed with distilled water three times and dried at 50 ^{o}C under a stream of N_2 gas.

Samples were analyzed by a 300 MHz Bruker AVANCE III NMR spectrometer equipped with a 4 mm magic angle spinning (MAS) probe (Bruker BioSpin, Billerica, MA) at Baylor

University (Waco, TX). Approximately 70 to 120 mg of sample was placed in a zirconium rotor with a diameter of 4 mm and Kel-F caps. Cross polarization spectra were applied with 5000 scans, a 2 ms contact time, at 12 kHz MAS frequency, and 1.2 s recycle delay. More ^{13}C NMR analytical details can be found in Cusack et al. (2018). Resulting spectra were divided into seven C functional groups, and the relative contributions were quantified by integrating the signal intensities of different chemical shift regions: 0–45 ppm assigned to alkyl C, 45–60 ppm to N-alkyl/methoxyl C (N-alkyl), 60–95 ppm to O-alkyl C, 95–110 ppm to di-O-alkyl C, 110–145 ppm to aromatic C, 145–165 ppm to phenolic C, and 165–215 ppm to amide/carboxyl C. The percentages of six biomolecular SOM constituents, including carbohydrate, protein, lignin, lipid, carbonyl and char, were estimated from the integrated spectra for each sample using a molecular mixing model constrained by C and N concentrations after the acid pre-treatment (Table S4) measured by combustion on an elemental analyzer (Baldock et al., 2004). The mass of each biomolecular SOM constituent was calculated by multiplying total C mass by its corresponding percentage as estimated above. The mass balance of each biomolecular SOM constituent after the 384-day incubation was also estimated by subtracting the mass remaining after the 384-day incubation from the initial mass at the beginning of the incubation. The nominal C oxidation state of each sample was calculated as the weighted average of different C functional groups following Hockaday et al. (2009).

Data analysis

The cumulative C mineralization, DOC in the sequential extractions, and C mass remaining from each biomolecular SOM component were expressed relative to initial total mass (5.5 g for each sample). For comparison between the two soils, we further calculated the percentage of total C loss (CO_2 + CH_4) to initial total C mass (415.2 mg C in the Oxisol amended with litter and 385.7 mg C in the Mollisol amended with litter) and the percentage of litter- and soil-C losses to their respective total organic C at the beginning of the incubation (191.2 mg C in litter, 224.0 mg C in the Oxisol and 175.5 mg C in the Mollisol for each sample). The differences in cumulative total-, litter- and soil-C mineralization and soil chemical properties between the aerobic and anaerobic

treatments in each soil were tested with Welch's *t*-test. Statistically significant differences were determined at $P < 0.05$, with $P < 0.10$ defined as marginally significant. Variation around the mean was reported as standard error. All analyses were conducted with the R statistical package (R Core Team, 2019).

Results

Cumulative total-, litter- and soil-C mineralization

Cumulative C mineralization ($CO_2 + CH_4$) from the aerobic treatment (control) was 27.4 ± 2.3% in the Oxisol and 25.8 ± 0.9% in the Mollisol, in terms of initial total C mass. Mineralization of C in the anaerobic treatment significantly decreased to 20.0 ± 0.2% in the Oxisol ($P < 0.05$) and 15.3 ± 0.2% in the Mollisol ($P < 0.01$). The anaerobic treatment had significantly less CO_2 production but more CH_4 emission in both soils during the incubation ($P < 0.01$; Fig. S3). The mean percent contribution of CH_4 to total C mineralization was significantly larger ($P < 0.01$) in the anaerobic treatment (41 ± 0% in the Oxisol and 34 ± 2% in the Mollisol) relative to the control (0.4 ± 0.1% in the Oxisol and 0.7 ± 0.3% in the Mollisol). Partitioning of total C losses ($CO_2 + CH_4$) based on the $\delta^{13}C$ values (Fig. S3 and S4) showed that the decreases in cumulative C mineralization in the anaerobic treatment were primarily due to depressed litter-C mineralization in both soils (Fig. 1).

The anaerobic treatment differentially affected litter- and soil-C mineralization in both the Oxisol and Mollisol. Expressed in terms of initial C mass, litter-C loss in the control was 45.0 ± 2.7% in the Oxisol and 45.5 ± 0.9% in the Mollisol, and significantly decreased to 30.5 ± 0.4% in the Oxisol and 17.8 ± 0.4% in the Mollisol under the anaerobic treatment ($P < 0.01$; Fig. 1). In contrast to litter-C, however, soil-C mineralization was not significantly depressed by anaerobiosis, and even slightly increased in the Mollisol (Fig. 1). Soil-C loss in the Oxisol was 12.4 ± 2.0% in the control and 11.0 ± 0.1% in the anaerobic treatment ($P = 0.51$), while soil-C loss in the Mollisol measured 5.3 ± 1.5% in the control and 12.5 ± 0.6% in the anaerobic treatment ($P < 0.01$). These conclusions were not substantially altered by selection of different litter $\delta^{13}C$ end-member values under anaerobic conditions (Table S3).

Soil Fe dynamics

The anaerobic treatment significantly increased net Fe reduction over the course of the experiment in both the Oxisol (14.3 mg Fe g^{-1}) and Mollisol (1.9 mg Fe g^{-1}) relative to the aerobic control. For the Oxisol, $Fe(II)_{HCl}$ concentrations in the control after the 384-day incubation (0.6 ± 0.2 mg g^{-1}) were similar to the initial values (0.6 ± 0.1 mg g^{-1}), but they were 25-fold greater ($P < 0.01$) in the anaerobic treatment (14.9 ± 0.4 mg g^{-1}) than the control (Fig. 2a). Oxisol $Fe(III)_{HCl}$ concentrations were 10-fold less ($P < 0.01$) in the anaerobic treatment (1.0 ± 0.3 mg g^{-1}) than the control (10.4 ± 1.6 mg g^{-1}). In the Mollisol, initial $Fe(II)_{HCl}$ concentrations were relatively high (1.8 ± 0.1 mg g^{-1}) due to wet conditions during soil sampling, but still increased two-fold ($P < 0.01$) under the anaerobic treatment (3.7 ± 0.1 mg g^{-1}) after 384 days relative to the control (1.8 ± 0.2 mg g^{-1}; Fig. 2b). Mollisol $Fe(III)_{HCl}$ was similar between the control (0.19 ± 0.03 mg g^{-1}) and anaerobic treatment (0.14 ± 0.04 mg g^{-1}). Overall, the anaerobic treatment significantly increased the 0.5 M HCl-extractable Fe ($Fe(II)_{HCl}$ + $Fe(III)_{HCl}$) in both the Oxisol ($P < 0.05$) and Mollisol ($P < 0.01$). The anaerobic treatment had no significant effects on Fe extracted by dithionite in either the Oxisol (45.0 ± 2.2 mg g^{-1}) or Mollisol (3.2 ± 0.2 mg g^{-1}; Fig. 2c, d), and comparison of Fe concentrations in the separate 0.5M HCl and dithionite extractions indicated that the latter mostly represented chemically reducible (as opposed to weak-acid-soluble) Fe(III) phases (Fig. 2). However, Fe extracted by pyrophosphate following extraction by dithionite was significantly affected by the anaerobic treatment in both soils. Pyrophosphate-extractable Fe decreased from 3.2 ± 1.0 mg g^{-1} in the control to 0.5 ± 0.07 mg g^{-1} in the anaerobic treatment in the Oxisol ($P = 0.05$), but increased from 1.6 ± 0.2 mg g^{-1} in the control to 4.8 ± 0.4 mg g^{-1} in the anaerobic treatment ($P < 0.01$) in the Mollisol. This resulted in significantly greater cumulative Fe extracted by dithionite and pyrophosphate ($P < 0.01$) in the anaerobic treatment (8.0 ± 0.5 mg g^{-1}) than in the control (4.8 ± 0.3 mg g^{-1}) in the Mollisol. Soil pH differed strongly between soils but was statistically similar between the control (5.51 ± 0.16 in the Oxisol and 8.45 ± 0.03 in the Mollisol) and the anaerobic treatment (6.09 ± 0.32 in the Oxisol and 8.67 ± 0.14 in the Mollisol).

Extractable organic C

The differences in the concentrations and $\delta^{13}C$ values of DOC between the treatments (Fig. S5) showed that anaerobic conditions significantly affected the sources of DOC in the sequential extraction solutions in both soils (Fig. 3). The anaerobic treatment often increased litter-derived DOC but decreased soil-derived DOC in soil extractions relative to the control (Fig. 3). In the Oxisol, soil-derived $DOC_{Na_4P_2O_7}$ was significantly smaller ($P < 0.01$) in the anaerobic treatment (5.8 ± 0.2 mg C g^{-1}) than the control (8.7 ± 0.3 mg C g^{-1}), while soil-derived DOC_{H_2O} was larger in the anaerobic treatment (1.1 ± 0.0 mg C g^{-1}) than the control (0.2 ± 0.0 mg C g^{-1}; $P < 0.01$). In the Mollisol, the anaerobic treatment had significantly less soil-derived DOC_{H_2O} (0.0 ± 0.0 mg C g^{-1}; $P < 0.01$), $DOC_{Na_2SO_4}$ (0.8 ± 0.2 mg C g^{-1};$P < 0.05$), and $DOC_{Na_2S_2O_4}$ (0.6 ± 0.1 mg C g^{-1}; $P < 0.01$) than the control (0.4 ± 0.1 mg C g^{-1} for DOC_{H_2O}, 1.5 ± 0.2 mg C g^{-1} for $DOC_{Na_2SO_4}$ and 1.4 ± 0.2 mg C g^{-1} for $DOC_{Na_2S_2O_4}$). On the other hand, litter-derived DOC_{H_2O} was significantly larger in the anaerobic treatment (0.5 ± 0.0 mg C g^{-1} in the Oxisol and 3.4 ± 0.4 mg C g^{-1} in the Mollisol) than the control (0.1 ± 0.0 mg C g^{-1} in the Oxisol and 0.5 ± 0.1 mg C g^{-1} in the Mollisol; $P < 0.01$). Litter-derived $DOC_{Na_2SO_4}$ was also significantly greater in the anaerobic treatment (2.1 ± 0.2 mg C g^{-1}) relative to the control (1.0 ± 0.1 mg C g^{-1}; $P < 0.01$) in the Mollisol. The anaerobic treatment did not have any significant effect on either litter-derived $DOC_{Na_2S_2O_4}$ or $DOC_{Na_4P_2O_7}$ in the Oxisol or Mollisol.

Biomolecular SOM constituents

The ^{13}C NMR analyses showed that the chemical compositions of SOC in both soils changed following the incubation (Table 1) and differed between the anaerobic treatment and the control (Fig. 4). Overall, both soils lost carbohydrate, lignin, lipid and char C, and gained protein and carbonyl C after the 384-day incubation, but the magnitude of these changes differed between treatments (Table 1). The anaerobic treatment significantly decreased the proportion of protein C in both the Oxisol ($22.6 \pm 0.1\%$ in the control vs. $19.2 \pm 0.3\%$ in the anaerobic treatment; $P < 0.01$)

and Mollisol (23.4 ± 0.3% in the control vs. 19.9 ± 0.6% in the anaerobic treatment; $P < 0.05$), as indicated by changes in N-alkyl and amide/carboxyl peak areas (Fig. 4). In contrast, carbohydrate C tended to be proportionally greater in the anaerobic treatment than the control in both the Oxisol (46.2 ± 0.9% vs. 42.8 ± 0.3%; $P = 0.09$) and Mollisol (31.1 ± 0.9% vs. 26.9 ± 1.1%; $P = 0.06$), as indicated by O-alkyl peak areas ($P = 0.06$ in the Oxisol and $P = 0.06$ in the Mollisol). In the Mollisol, the proportion of lignin also tended to be larger in the anaerobic treatment (15.8 ± 0.2%) relative to the control (14.4 ± 0.3%; $P = 0.07$). The proportion of lignin in the Oxisol measured 18.9 ± 0.3% in the anaerobic treatment and 18.1 ± 0.3% in the control, but the difference was not significant ($P = 0.18$). The C compositional differences between treatments largely remained consistent when accounting for differences in total C mass remaining and expressing molecular C components on a mass basis (Fig. 4g, h). The anaerobic treatment significantly decreased the accumulation of protein C mass in the Oxisol ($P < 0.05$), and it significantly depressed the loss of carbohydrate and lignin C mass in both the Oxisol ($P < 0.01$) and Mollisol ($P < 0.05$) (Fig. 4g, h and Table 1). The oxidation state of organic C in both soils was near zero before and after the incubation (Table 1). At the end of the experiment, the anaerobic treatment had a slightly lower C oxidation state (-0.156 in the Oxisol and -0.013 in the Mollisol) than the control (-0.144 in the Oxisol and 0.031 in the Mollisol), consistent with a preferential loss of oxidized C.

Discussion

Our data were consistent with our first hypothesis: decomposition of soil C was less sensitive to anoxia than decomposition of litter C as a consequence of release (Fig. 3) and mineralization (Fig. 1) of physico-chemically protected C, which was likely driven by Fe reduction (Fig. 2). The anaerobic treatments consistently suppressed total C mineralization by 27% in the Oxisol and by 41% in the Mollisol due to their decreases in litter-C mineralization (30.5% vs. 45.0% in the control in the Oxisol and 17.8% vs. 45.5% in the control in the Mollisol, in terms of initial C mass). However, we did not observe a significant net suppression of soil-C decomposition due to anaerobiosis after one year (11.0% in the anaerobic treatment and 12.4% in the control in the

Oxisol; 12.5% in the anaerobic treatment and 5.3% in the control in the Mollisol). The sustained or slightly higher decomposition of soil C and suppressed decomposition of litter C under anaerobic conditions were linked to changes in C molecular composition. In partial support of our second hypothesis, anaerobic conditions significantly decreased the accumulation of protein C (Fig. 4e, f), which generally has a C nominal oxidation state between -1.0 and 1.5 and is thermodynamically favorable for decomposition in the absence of O_2 if Fe(III) is present (Keiluweit et al., 2016; LaRowe & Van Cappellen, 2011). We also found that lignin decomposition tended to be suppressed under anaerobic conditions, consistent with previous evidence that O_2 is necessary for depolymerization of macromolecular lignin (Benner & Maccubbin, 1984; Freeman et al., 2001; Kirk & Farrell, 1987). However, we also observed a decrease in carbohydrate decomposition under anaerobic conditions (Fig. 4g, h), despite its vulnerability to hydrolysis and its relatively high C nominal oxidation state (-1.0 to 1.0). This finding may have reflected the protective encasement of cellulose and hemicellulose by lignin in the added litter (Kirk & Farrell, 1987).

Tradeoffs in SOM protection mechanisms

Anaerobic conditions are traditionally thought to suppress organic matter decomposition due to kinetic constraints on extracellular enzyme activity and thermodynamic constraints on microbial metabolism (Boye et al., 2017; Freeman et al., 2001; Greenwood, 1961; Keiluweit et al., 2016; McLatchey & Reddy, 1998). In the two disparate soils examined here, we found that this long-standing theory was applicable to the mineralization of litter C but not soil C, which had similar or slightly higher C loss in the anaerobic treatments compared with the control (Fig. 1). The different responses of soil- vs. litter-C mineralization to anaerobic conditions, along with the greater loss of soil-derived DOC in the sequential extractions under the anaerobic treatment (Fig. 3), thus indicate the disruption of C protection mechanism(s) that allowed decomposition of soil C to continue apace even as litter decomposition was suppressed.

Accordingly, the results from the sequential extractions revealed that the mineral-associated soil C released following Fe reduction likely contributed to the sustained soil C decomposition under O_2 limitation. Increased losses of soil-derived DOC from mineral associations in the anaerobic than aerobic treatments (Fig. 3) indicated that more extant soil C was released and then subjected to anaerobic respiration. In upland soils, associations with Fe oxides may protect C against microbial attack (Wagai & Mayer, 2007). However, anoxia may cause portions of this Fe-bound organic C to be released following Fe reduction (Buettner et al., 2014; Thompson, Chadwick, Boman, & Chorover, 2006), and thus more susceptible to microbial attack. Greater net Fe reduction (14.3 mg Fe g^{-1} for the Oxisol and 1.9 mg Fe g^{-1} for the Mollisol) but little change in pH under the anaerobic treatment suggest the importance of reductive dissolution of Fe oxides rather than pH-mediated changes in mineral surface charge in controlling C release in this study (Pan et al., 2016). However, portions of the released soil-C may consist of C components protected by kinetic or thermodynamic constraints, as discussed below, which resulted in accumulation of soil-derived DOC_{H_2O} under anaerobic conditions (Fig. 3a).

Intriguingly, litter C in DOC_{H_2O} and $DOC_{Na_2SO_4}$ accumulated under anaerobic conditions to a much greater extent in the Mollisol (10-fold) than the Oxisol. This may reflect lower overall availability of terminal electron acceptors, especially Fe, in the Mollisol (55-fold less of $Fe(III)_{HCl}$ than the Oxisol; Fig. 2), leading to increased thermodynamic limitation on the metabolism of soluble C (Keiluweit et al., 2016; LaRowe & Van Cappellen, 2011). Nitrate concentrations in the initial soils were small (1.06 μmol g^{-1} in the Oxisol and 2.09 μmol g^{-1} in the Mollisol; Table S1) relative to the increases in $Fe(II)_{HCl}$ under the anaerobic treatment after 384-day incubation (Fig. 2). Nitrate could not be replenished by aerobic nitrification under the anaerobic treatment, and thus differences in nitrate availability as a terminal electron acceptor between the two soils contributed negligibly to their responses of litter-derived DOC to anoxia.

Moreover, in addition to promoting Fe reduction, we note that the anaerobic treatment altered the distribution of soil Fe among the different extractable pools. These indicate that anoxia

altered Fe(III) phase composition and crystallinity (Winkler et al., 2018), which could potentially disrupt mineral-organic C associations. The anaerobic treatment significantly increased total Fe in the 0.5 M HCl extraction in both soils, while also significantly increasing total Fe in the dithionite + pyrophosphate extractions in the Mollisol (there was a similar but nonsignificant trend in the Oxisol; Fig. 2). This intriguing finding is consistent with alteration of soil microaggregation by reductive dissolution of Fe-oxide cements, which are known to contribute to aggregate stability (Barral et al., 1998). Some Fe(III) phases and organo-Fe co-precipitates can be shielded within aggregates and/or by other minerals (Filimonova et al., 2016). Thus, Fe reduction could expose previously protected Fe to the extractant solutions, explaining the observed increase in Fe concentrations. This would also promote the dispersion and release of mineral and organic colloids that were previously protected within aggregates (Tadanier, Schreiber, & Roller, 2005; Thompson, Chadwick, Boman, & Chorover, 2006). Thus, our data are consistent with both the direct and indirect release of physico-chemically protected C as a consequence of Fe reduction.

Preferential accrual of specific C forms under anaerobic conditions

Comparing SOC chemical composition measured by ^{13}C NMR before and after the incubation showed that total mineralized C in both soils was largely derived from carbohydrates (Table 1). There was also a small amount of lignin, lipid and char C loss due to decomposition, as well as small gain in carbonyl C which was likely derived from oxidized litter decomposition products (Table 1). The small observed gains of protein C after incubation likely reflect the balance between losses of these components from decomposition of extant SOM and their production during the incubation as a consequence of microbial biomass growth on decomposing litter (Kallenbach et al., 2016). The fact that the net gain of protein C was smaller under anaerobic than aerobic conditions could thus be due either to greater losses from SOM, and/or smaller production of protein from microbial sources as a consequence of lower litter decomposition. We note the caveat that acid pretreatment is a widely established method for removing interfering elements and concentrating SOM prior to NMR analysis, but it leads to losses of acid-soluble SOM

moieties—particularly carbohydrates (Cusack et al., 2018; Gélinas et al., 2001; Schmidt et al., 1997). As such, our inference from the NMR data is restricted to HF-insoluble soil C. However, since the same pretreatment was applied to all samples, we can make robust comparisons among treatments before and after incubation.

Overall, the decreased protein-derived C but increased lignin- and carbohydrate-C under the anerobic vs. aerobic treatments at the end of experiment indicated the selective accrual and losses of specific C components due to O_2 limitation. The mineral-associated soil C which was released under anaerobic conditions and subsequently oxidized (Figs. 1 and 3) likely contained a significant protein component (Table 1, Fig. 4). Previous studies have posited that relatively oxidized organic C forms such as proteins (C nominal oxidation state > -1) are more favorable for decomposition than more reduced organic C forms (e.g., lipids with nominal oxidation state < -1) in the absence of O_2 due to thermodynamic inhibition (Keiluweit et al., 2016; LaRowe & Van Cappellen, 2011). Thus, the observed release and metabolism of proteins following Fe reduction is consistent with thermodynamic constraints. Intriguingly, we did not observe preferential protection of lipids under anaerobic conditions in our study, in contrast to other studies (Keiluweit et al., 2017; LaCroix et al., 2019). The lipid C inputs from the added litter (0.80 mg C g^{-1}) measured about half of the mean net loss of lipid C during the incubation (1.75 mg C g^{-1} in the Oxisol and 1.55 mg C g^{-1} in the Mollisol). Microbial biomass growth can provide a significant source of lipids to soil (Kallenbach et al., 2016; Wang et al., 2015), and microbial biomass often declines under anaerobic conditions (McLatchey & Reddy, 1998; Ye et al., 2019). The lack of decreased lipid loss in the anaerobic treatment might result from the combination of suppressed decomposition of lipids from litter and soil combined with lesser lipid production in microbial biomass as a consequence of slower anaerobic litter decomposition (Fig. 1).

Lignin and carbohydrate C were preferentially retained in soils under anaerobic conditions, consistent with another recent study (Dao et al., 2018). Sustained anoxia can suppress lignin decomposition by limiting the activity of oxidative enzymes and production of reactive oxygen species, both of which require O_2 (Benner & Maccubbin, 1984; Kirk & Farrell, 1987). Although

carbohydrates can be readily depolymerized and oxidized under anaerobic conditions, suppressed carbohydrate-C decomposition might have occurred due to the encasement of celluloses and/or hemicelluloses in lignin, which physically shielded them from hydrolytic attack on the added litter (Kirk & Farrell, 1987). Furthermore, lignin derivatives in SOM have been shown to be preferentially adsorbed and/or coprecipitated by Fe minerals relative to other organic compounds (Coward et al., 2018; Huang et al., 2019; Kramer et al., 2012; Wang et al., 2017), and less readily liberated from mineral associations by reductive dissolution (Han et al., 2019; Mejia et al., 2018). Our data (Table 1, Fig. 4) are thus consistent with the importance of both plant- and microbial-derived C forms as SOM components in redox-dynamic mineral soils.

Conclusion

Our results demonstrate a tradeoff in C protection mechanisms and molecular composition under aerobic vs. anaerobic conditions which was consistent across two dramatically different mineral soils. Anoxia suppressed total C loss from both soils by decreasing litter decomposition while sustaining or slightly increasing native soil C decomposition. Relatively oxidized C compounds such as proteins may be released following Fe reduction and decomposed anaerobically, which may offset the decreased decomposition of other C compounds (such as lignin and associated carbohydrates) where decomposition may be kinetically or thermodynamically inhibited in the absence of O_2. Anaerobic microsites may be ubiquitous in soil and are likely to vary dynamically as a function of soil moisture, aggregate size distributions, soil texture, and C supply and demand (Hall & Silver, 2015; Keiluweit et al., 2016, 2018; Sexstone et al., 1985). Soil O_2 availability is also likely to be significantly affected by global change given its link to soil moisture and precipitation (Liptzin et al., 2011) and the increased prevalence of extreme precipitation events and droughts (e.g., Min, Zhang, Zwiers, & Hegerl, 2011; O'Connell et al., 2018). Thus, the O_2-linked tradeoffs in soil C protection mechanisms identified in this study are likely to be broadly important across ecosystems, especially in response to global change. Current soil C cycling models representing the effects of anaerobic conditions on C oxidation typically assume that SOM

decomposition rate decreases severely when O_2 declines (Koven et al., 2013; Riley et al., 2011). However, as demonstrated by our study, SOM decomposition may be sustained under anaerobic conditions due to compensatory mechanisms such as the release and metabolism of mineral-associated C. This should not be overlooked, especially given that Fe-associated pools and mineral-associated C in general, represent a large fraction of soil C among ecosystems (von Lützow et al., 2007; Zhao et al., 2016). Incorporation of the coupled and contrasting biological and geochemical impacts of O_2 limitation on decomposition identified here may be key for improving model predictions of soil C dynamics under a warmer and wetter future climate.

Acknowledgements

This research was supported in part by NSF grant DEB-1457805 and the Luquillo Critical Zone Observatory (EAR-1331841). We thank Anthony Mirabito for assistance in the lab.

Conflicts of interest

The authors declare no conflicts of interest

Data accessibility

The data that support the findings of this study are available from the authors upon reasonable request.

References

Amundson, R. G., Trask, J., & Pendall, E. (1988). A rapid method of soil carbonate analysis using gas chromatography. *Soil Science Society of America Journal*, *52*(3), 880–883. https://doi.org/10.2136/sssaj1988.03615995005200030050x

Arndt, S., Jørgensen, B. B., LaRowe, D. E., Middelburg, J. J., Pancost, R. D., & Regnier, P. (2013). Quantifying the degradation of organic matter in marine sediments: A review and synthesis. *Earth-Science Reviews*, *123*, 53–86.

https://doi.org/10.1016/j.earscirev.2013.02.008

Baldock, J. A., Masiello, C. A., Gélinas, Y., & Hedges, J. I. (2004). Cycling and composition of organic matter in terrestrial and marine ecosystems. *Marine Chemistry*, *92*(1), 39–64. https://doi.org/10.1016/j.marchem.2004.06.016

Barral, M. T., Arias, M., & Guérif, J. (1998). Effects of iron and organic matter on the porosity and structural stability of soil aggregates. *Soil and Tillage Research*, *46*(3), 261–272. https://doi.org/10.1016/S0167-1987(98)00092-0

Benner, R., & Maccubbin, A. E. (1984). Anaerobic biodegradation of the lignin and polysaccharide components of lignocellulose and synthetic lignin by sediment microflorat. *Applied and Environmental Microbiology*, *47*(5), 998–1004.

Bowling, D. R., Pataki, D. E., & Randerson, J. T. (2008). Carbon isotopes in terrestrial ecosystem pools and CO_2 fluxes. *New Phytologist*, *178*(1), 24–40. https://doi.org/10.1111/j.1469-8137.2007.02342.x

Boye, K., Noël, V., Tfaily, M. M., Bone, S. E., Williams, K. H., Bargar, J. R., & Fendorf, S. (2017). Thermodynamically controlled preservation of organic carbon in floodplains. *Nature Geoscience*, *10*(6), 415–419. https://doi.org/10.1038/ngeo2940

Breecker, D. O., Bergel, S., Nadel, M., Tremblay, M. M., Osuna-Orozco, R., Larson, T. E., & Sharp, Z. D. (2015). Minor stable carbon isotope fractionation between respired carbon dioxide and bulk soil organic matter during laboratory incubation of topsoil. *Biogeochemistry*, *123*(1–2), 83–98. https://doi.org/10.1007/s10533-014-0054-3

Buettner, S. W., Kramer, M. G., Chadwick, O. A., & Thompson, A. (2014). Mobilization of colloidal carbon during iron reduction in basaltic soils. *Geoderma*, *221–222*, 139–145. https://doi.org/10.1016/j.geoderma.2014.01.012

Chen, C., Meile, C., Wilmoth, J., Barcellos, D., & Thompson, A. (2018). Influence of pO_2 on iron redox cycling and anaerobic organic carbon mineralization in a humid tropical forest soil. *Environmental Science & Technology*, *52*(14), 7709–7719. https://doi.org/10.1021/acs.est.8b01368

Coward, E. K., Ohno, T., & Plante, A. F. (2018). Adsorption and molecular fractionation of dissolved organic matter on iron-bearing mineral matrices of varying crystallinity. *Environmental Science & Technology*, *52*(3), 1036–1044. https://doi.org/10.1021/acs.est.7b04953

Cusack, D. F., Halterman, S. M., Tanner, E. V. J., Wright, S. J., Hockaday, W., Dietterich, L. H., & Turner, B. L. (2018). Decadal-scale litter manipulation alters the biochemical and physical character of tropical forest soil carbon. *Soil Biology and Biochemistry*, *124*, 199–209. https://doi.org/10.1016/j.soilbio.2018.06.005

Dao, T. T., Gentsch, N., Mikutta, R., Sauheitl, L., Shibistova, O., Wild, B., Schnecker, J., Bárta, J., Čapek, P., Gittel, A., Lashchinskiy, N., Urich, T., Šantrůčková, H., Richter, A., & Guggenberger, G. (2018). Fate of carbohydrates and lignin in north-east Siberian permafrost soils. *Soil Biology and Biochemistry*, *116*, 311–322. https://doi.org/10.1016/j.soilbio.2017.10.032

Ehleringer, J. R., Buchmann, N., & Flanagan, L. B. (2000). Carbon isotope ratios in belowground carbon cycle processes. *Ecological Applications*, *10*(2), 412–422. https://doi.org/10.1890/1051-0761(2000)010[0412:CIRIBC]2.0.CO;2

Filimonova, S., Kaufhold, S., Wagner, F. E., Häusler, W., & Kögel-Knabner, I. (2016). The role of allophane nano-structure and Fe oxide speciation for hosting soil organic matter in an allophanic Andosol. *Geochimica et Cosmochimica Acta*, *180*, 284–302. https://doi.org/10.1016/j.gca.2016.02.033

Freeman, C., Ostle, N., & Kang, H. (2001). An enzymic "latch" on a global carbon store. *Nature*, *409*, 149.

Gao, H., Chen, X., Wei, J., Zhang, Y., Zhang, L., Chang, J., & Thompson, M. L. (2016). Decomposition dynamics and changes in chemical composition of wheat straw residue under anaerobic and aerobic conditions. *PLOS ONE*, *11*(7), e0158172. https://doi.org/10.1371/journal.pone.0158172

Gélinas, Y., Baldock, J. A., & Hedges, J. I. (2001). Demineralization of marine and freshwater

sediments for CP/MAS ^{13}C NMR analysis. *Organic Geochemistry*, *32*(5), 677–693. https://doi.org/10.1016/S0146-6380(01)00018-3

Greenwood, D. J. (1961). The effect of oxygen concentration on the decomposition of organic materials in soil. *Plant and Soil*, *14*(4), 360–376. https://doi.org/10.1007/BF01666294

Hagedorn, F., Kaiser, K., Feyen, H., & Schleppi, P. (2000). Effects of redox conditions and flow processes on the mobility of dissolved organic carbon and nitrogen in a forest soil. *Journal of Environmental Quality*, *29*(1), 288–297. https://doi.org/10.2134/jeq2000.00472425002900010036x

Hall, S. J., Baker, M. A., Jones, S. B., Stark, J. M., & Bowling, D. R. (2016). Contrasting soil nitrogen dynamics across a montane meadow and urban lawn in a semi-arid watershed. *Urban Ecosystems*, *19*(3), 1083–1101. https://doi.org/10.1007/s11252-016-0538-0

Hall, S. J., Huang, W., & Hammel, K. E. (2017). An optical method for carbon dioxide isotopes and mole fractions in small gas samples: Tracing microbial respiration from soil, litter, and lignin. *Rapid Communications in Mass Spectrometry*, *31*(22), 1938–1946. https://doi.org/10.1002/rcm.7973

Hall, S. J., & Silver, W. L. (2015). Reducing conditions, reactive metals, and their interactions can explain spatial patterns of surface soil carbon in a humid tropical forest. *Biogeochemistry*, *125*(2), 149–165. https://doi.org/10.1007/s10533-015-0120-5

Hall, S. J., Treffkorn, J., & Silver, W. L. (2014). Breaking the enzymatic latch: impacts of reducing conditions on hydrolytic enzyme activity in tropical forest soils. *Ecology*, *95*(10), 2964–2973. https://doi.org/10.1890/13-2151.1

Han, L., Sun, K., Keiluweit, M., Yang, Y., Yang, Y., Jin, J., Sun, H., Wu, F., & Xing, B. (2019). Mobilization of ferrihydrite-associated organic carbon during Fe reduction: Adsorption versus coprecipitation. *Chemical Geology*, *503*, 61–68. https://doi.org/10.1016/j.chemgeo.2018.10.028

Hockaday, W. C., Masiello, C. A., Randerson, J. T., Smernik, R. J., Baldock, J. A., Chadwick, O. A., & Harden, J. W. (2009). Measurement of soil carbon oxidation state and oxidative ratio

by ^{13}C nuclear magnetic resonance. *Journal of Geophysical Research: Biogeosciences*, *114*(G2). https://doi.org/10.1029/2008JG000803

Huang, W., & Hall, S. J. (2017a). Optimized high-throughput methods for quantifying iron biogeochemical dynamics in soil. *Geoderma*, *306*, 67–72. https://doi.org/10.1016/j.geoderma.2017.07.013

Huang, W., & Hall, S. J. (2017b). Elevated moisture stimulates carbon loss from mineral soils by releasing protected organic matter. *Nature Communications*, *8*, 1774. https://doi.org/10.1038/s41467-017-01998-z

Huang, W., & Hall, S. J. (2018). Large impacts of small methane fluxes on carbon isotope values of soil respiration. *Soil Biology and Biochemistry*, *124*, 126–133. https://doi.org/10.1016/j.soilbio.2018.06.003

Huang, W., Hammel, K. E., Hao, J., Thompson, A., Timokhin, V. I., & Hall, S. J. (2019). Enrichment of lignin-derived carbon in mineral-associated soil organic matter. *Environmental Science & Technology*, *53*(13), 7522–7531. https://doi.org/10.1021/acs.est.9b01834

Kaiser, K., Guggenberger, G., & Zech, W. (2001). Isotopic fractionation of dissolved organic carbon in shallow forest soils as affected by sorption. *European Journal of Soil Science*, *52*(4), 585–597. https://doi.org/10.1046/j.1365-2389.2001.00407.x

Kallenbach, C. M., Frey, S. D., & Grandy, A. S. (2016). Direct evidence for microbial-derived soil organic matter formation and its ecophysiological controls. *Nature Communications*, *7*, 13630. https://doi.org/10.1038/ncomms13630

Keiluweit, M., Gee, K., Denney, A., & Fendorf, S. (2018). Anoxic microsites in upland soils dominantly controlled by clay content. *Soil Biology and Biochemistry*, *118*, 42–50. https://doi.org/10.1016/j.soilbio.2017.12.002

Keiluweit, M., Nico, P. S., Kleber, M., & Fendorf, S. (2016). Are oxygen limitations under recognized regulators of organic carbon turnover in upland soils? *Biogeochemistry*, *127*(2–3), 157–171. https://doi.org/10.1007/s10533-015-0180-6

Keiluweit, M., Wanzek, T., Kleber, M., Nico, P., & Fendorf, S. (2017). Anaerobic microsites have an unaccounted role in soil carbon stabilization. *Nature Communications*, *8*(1), 1771. https://doi.org/10.1038/s41467-017-01406-6

Kirk, T. K., & Farrell, R. L. (1987). Enzymatic "combustion": the microbial degradation of lignin. *Annual Review of Microbiology (USA)*, *41*, 465–505. https://doi-org.proxy.lib.iastate.edu/10.1146/annurev.mi.41.100187.002341

Kleber, M., Eusterhues, K., Keiluweit, M., Mikutta, C., Mikutta, R., & Nico, P. S. (2015). Mineral–organic associations: formation, properties, and relevance in soil environments. *Advances in Agronomy*, *130*, 1–140.

Koven, C. D., Riley, W. J., Subin, Z. M., Tang, J. Y., Torn, M. S., Collins, W. D., Bonan, G. B., Lawrence, D. M., & Swenson, S. C. (2013). The effect of vertically resolved soil biogeochemistry and alternate soil C and N models on C dynamics of CLM4. *Biogeosciences*, *10*(11), 7109–7131. https://doi.org/10.5194/bg-10-7109-2013

Kramer, M. G., Sanderman, J., Chadwick, O. A., Chorover, J., & Vitousek, P. M. (2012). Long-term carbon storage through retention of dissolved aromatic acids by reactive particles in soil. *Global Change Biology*, *18*(8), 2594–2605. https://doi.org/10.1111/j.1365-2486.2012.02681.x

Krichels, A., DeLucia, E. H., Sanford, R., Chee-Sanford, J., & Yang, W. H. (2019). Historical soil drainage mediates the response of soil greenhouse gas emissions to intense precipitation events. *Biogeochemistry*, *142*(3), 425–442. https://doi.org/10.1007/s10533-019-00544-x

LaCroix, R. E., Tfaily, M. M., McCreight, M., Jones, M. E., Spokas, L., & Keiluweit, M. (2019). Shifting mineral and redox controls on carbon cycling in seasonally flooded mineral soils. *Biogeosciences*, *16*(13), 2573–2589. https://doi.org/10.5194/bg-16-2573-2019

Lang, S. Q., Bernasconi, S. M., & Früh-Green, G. L. (2012). Stable isotope analysis of organic carbon in small (μg C) samples and dissolved organic matter using a GasBench preparation device. *Rapid Communications in Mass Spectrometry*, *26*(1), 9–16. https://doi.org/10.1002/rcm.5287

LaRowe, D. E., & Van Cappellen, P. (2011). Degradation of natural organic matter: A thermodynamic analysis. *Geochimica et Cosmochimica Acta*, *75*(8), 2030–2042. https://doi.org/10.1016/j.gca.2011.01.020

Liptzin, D., Silver, W. L., & Detto, M. (2011). Temporal dynamics in soil oxygen and greenhouse gases in two humid tropical forests. *Ecosystems*, *14*, 171–182. https://doi.org/10.1007/s10021-010-9402-x

McLatchey, G. P., & Reddy, K. R. (1998). Regulation of organic matter decomposition and nutrient release in a wetland soil. *Journal of Environment Quality*, *27*(5), 1268. https://doi.org/10.2134/jeq1998.00472425002700050036x

Mejia, J., He, S., Yang, Y., Ginder-Vogel, M., & Roden, E. E. (2018). Stability of ferrihydrite–humic acid coprecipitates under iron-reducing conditions. *Environmental Science & Technology*, *52*(22), 13174–13183. https://doi.org/10.1021/acs.est.8b03615

Min, S.-K., Zhang, X., Zwiers, F. W., & Hegerl, G. C. (2011). Human contribution to more-intense precipitation extremes. *Nature*, *470*(7334), 378–381. https://doi.org/10.1038/nature09763

Moyes, A. B., & Bowling, D. R. (2013). Interannual variation in seasonal drivers of soil respiration in a semi-arid Rocky Mountain meadow. *Biogeochemistry*, *113*(1–3), 683–697. https://doi.org/10.1007/s10533-012-9797-x

O'Connell, C. S., Ruan, L., & Silver, W. L. (2018). Drought drives rapid shifts in tropical rainforest soil biogeochemistry and greenhouse gas emissions. *Nature Communications*, *9*(1), 1348. https://doi.org/10.1038/s41467-018-03352-3

Pan, W., Kan, J., Inamdar, S., Chen, C., & Sparks, D. (2016). Dissimilatory microbial iron reduction release DOC (dissolved organic carbon) from carbon-ferrihydrite association. *Soil Biology and Biochemistry*, *103*, 232–240. https://doi.org/10.1016/j.soilbio.2016.08.026

R Core Team. (2019). *R: A Language and Environment for Statistical Computing*. R Foundation for Statistical Computing. https://www.R-project.org/

Riley, W. J., Subin, Z. M., Lawrence, D. M., Swenson, S. C., Torn, M. S., Meng, L., Mahowald, N. M., & Hess, P. (2011). Barriers to predicting changes in global terrestrial methane fluxes: analyses using CLM4Me, a methane biogeochemistry model integrated in CESM. *Biogeosciences*, *8*(7), 1925–1953. https://doi.org/10.5194/bg-8-1925-2011

Schmidt, M. W. I., Knicker, H., Hatcher, P. G., & Kogel-Knabner, I. (1997). Improvement of 13C and 15N CPMAS NMR spectra of bulk soils, particle size fractions and organic material by treatment with 10% hydrofluoric acid. *European Journal of Soil Science*, *48*(2), 319–328. https://doi.org/10.1111/j.1365-2389.1997.tb00552.x

Sexstone, A., Revsbech, N., Parkin, T., & Tiedje, J. (1985). Direct measurement of oxygen profiles and denitrification rates in soil aggregates. *Soil Science Society of America Journal*, *49*, 645–651.

Silver, W. L., Lugo, A. E., & Keller, M. (1999). Soil oxygen availability and biogeochemistry along rainfall and topographic gradients in upland wet tropical forest soils. *Biogeochemistry*, *44*(3), 301–328. https://doi.org/10.1023/A:1006034126698

Tadanier, C. J., Schreiber, M. E., & Roller, J. W. (2005). Arsenic mobilization through microbially mediated deflocculation of ferrihydrite. *Environmental Science & Technology*, *39*(9), 3061–3068. https://doi.org/10.1021/es048206d

Thompson, A., Chadwick, O. A., Boman, S., & Chorover, J. (2006). Colloid mobilization during soil iron redox oscillations. *Environmental Science & Technology*, *40*(18), 5743–5749. https://doi.org/10.1021/es061203b

von Fischer, J. C., & Hedin, L. O. (2007). Controls on soil methane fluxes: Tests of biophysical mechanisms using stable isotope tracers. *Global Biogeochemical Cycles*, *21*(2), GB2007. https://doi.org/10.1029/2006GB002687

von Lützow, M., Kögel-Knabner, I., Ekschmitt, K., Flessa, H., Guggenberger, G., Matzner, E., & Marschner, B. (2007). SOM fractionation methods: Relevance to functional pools and to stabilization mechanisms. *Soil Biology and Biochemistry*, *39*(9), 2183–2207. https://doi.org/10.1016/j.soilbio.2007.03.007

Wagai, R., & Mayer, L. M. (2007). Sorptive stabilization of organic matter in soils by hydrous iron oxides. *Geochimica et Cosmochimica Acta*, *71*(1), 25–35. https://doi.org/10.1016/j.gca.2006.08.047

Wang, H., Liu, S., Chang, S. X., Wang, J., Shi, Z., Huang, X., Wen, Y., Lu, L., & Cai, D. (2015). Soil microbial community composition rather than litter quality is linked with soil organic carbon chemical composition in plantations in subtropical China. *Journal of Soils and Sediments*, *15*(5), 1094–1103. https://doi.org/10.1007/s11368-015-1118-2

Wang, Y., Wang, H., He, J.-S., & Feng, X. (2017). Iron-mediated soil carbon response to water-table decline in an alpine wetland. *Nature Communications*, *8*, 15972. https://doi.org/10.1038/ncomms15972

Winkler, P., Kaiser, K., Thompson, A., Kalbitz, K., Fiedler, S., & Jahn, R. (2018). Contrasting evolution of iron phase composition in soils exposed to redox fluctuations. *Geochimica et Cosmochimica Acta*, *235*, 89–102. https://doi.org/10.1016/j.gca.2018.05.019

Ye, C., Hall, S. J., & Hu, S. (2019). Controls on mineral-associated organic matter formation in a degraded Oxisol. *Geoderma*, *338*, 383–392. https://doi.org/10.1016/j.geoderma.2018.12.011

Zhao, Q., Poulson, S. R., Obrist, D., Sumaila, S., Dynes, J. J., McBeth, J. M., & Yang, Y. (2016). Iron-bound organic carbon in forest soils: quantification and characterization. *Biogeosciences*, *13*(16), 4777–4788. https://doi.org/10.5194/bg-13-4777-2016

Table 1 Mass balance of six biomolecular SOM constituents in the Oxisol and Mollisol incubated under the aerobic (control) and anaerobic treatments after 384 days. The mass balance is reported relative to the initial sample mass.

	Initial C (mg C g^{-1} soil)		C loss (mg C g^{-1} soil)			
			Control		Anaerobic	
C components	Oxisol	Mollisol	Oxisol	Mollisol	Oxisol	Mollisol
Carbohydrate	38.77	27.87	15.31	14.82	10.84	10.45
Protein	9.18	9.07	-3.18[1]	-2.28	-2.47	-2.03
Lignin	15.99	11.47	6.10	4.49	4.58	2.63
Lipid	6.11	5.24	1.84	1.93	1.66	1.17
Carbonyl	0.54	1.41	-1.03	-2.52	-0.51	-2.22
Char	4.89	11.60	1.65	1.65	0.98	0.74
C oxidation state[2]	-0.150	-0.048	-0.144	0.031	-0.156	-0.013

[1]Negative values indicate a net gain of the respective C molecule

[2]Calculated after Hockaday et al. (2009); the Control and Anaerobic columns list the C oxidation state at the end of the experiment (not the change in C oxidation state)

Figure legends

Fig. 1 Total litter- and soil-C losses by mineralization to CO_2 and CH_4 from the Oxisol and Mollisol under the aerobic (control) and anaerobic treatments after 384 days. Carbon losses from litter and soil are expressed relative to initial C concentrations of the respective C sources. Isotope mixing models were used to partition total C losses from litter and soil sources as described in the Methods. ** indicates significant differences between the treatment and control at $P < 0.01$. Error bars indicate standard errors of incubation replicates (n = 5).

Fig. 2 Soil extractable Fe in the Oxisol and Mollisol under the aerobic (control) and anaerobic treatments after 384 days (note the different y-axis scales between soils). (a,b) Fe(II) and Fe(III) in 0.5M HCl. (c,d) Fe in sequential sodium dithionite and sodium pyrophosphate extractions. Different lowercase or uppercase letters indicate significant differences between the treatments at $P < 0.05$. Error bars indicate standard errors (n = 5).

Fig. 3 Litter- and soil-derived dissolved organic carbon (DOC) in sequential extractions (plotted in descending order by panel) of Oxisol and Mollisol samples from the aerobic (control) and anaerobic treatments after 384 days. The values are expressed relative to the initial sample masses. * and ** indicate significant differences between the treatment and control at $P < 0.05$ and 0.01, respectively. Error bars indicate standard errors (n = 5).

Fig. 4 Representative ^{13}C NMR spectra (a, b) and results from the ^{13}C NMR molecular mixing model. (a, b) representative ^{13}C NMR spectra from one replicate for each treatment in the Oxisol and Mollisol; (c, d) the percentages of seven C functional groups in the Oxisol and Mollisol; (e, f) the percentages of six biomolecular SOM constituents in the Oxisol and Mollisol; (g, h) estimated C mass remaining of six biomolecular SOM constituents relative to the initial sample mass in the Oxisol and Mollisol. * and ** indicate significant differences between the treatment and control at

$P < 0.05$ and 0.01, respectively. Error bars indicate standard errors (n = 2 for the control and n = 3 for the anaerobic treatment).

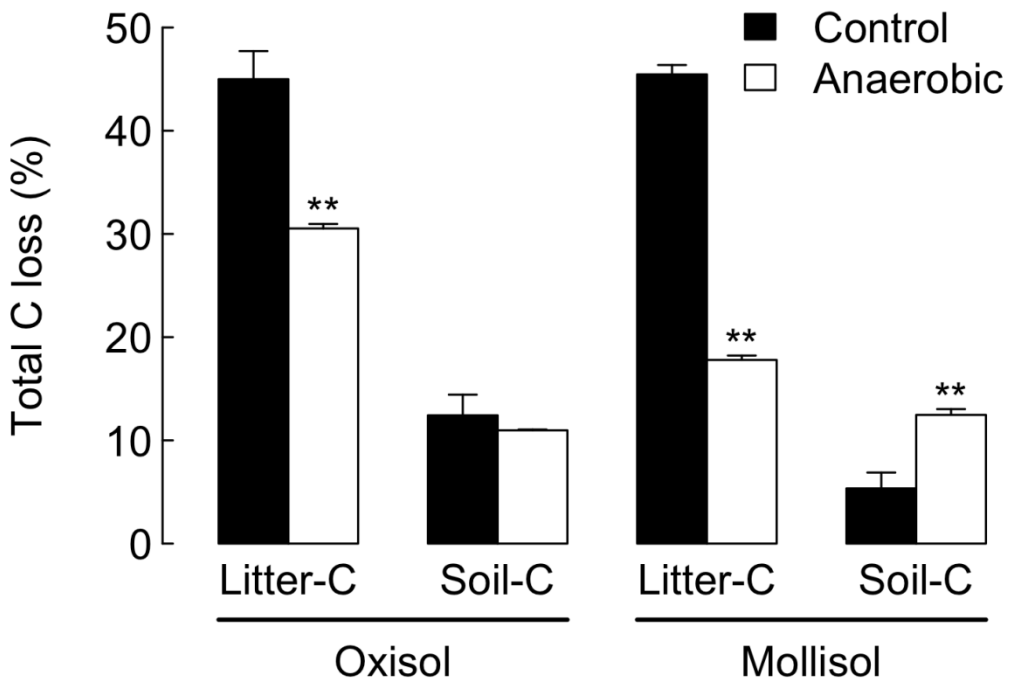

gcb_15100_f1.png

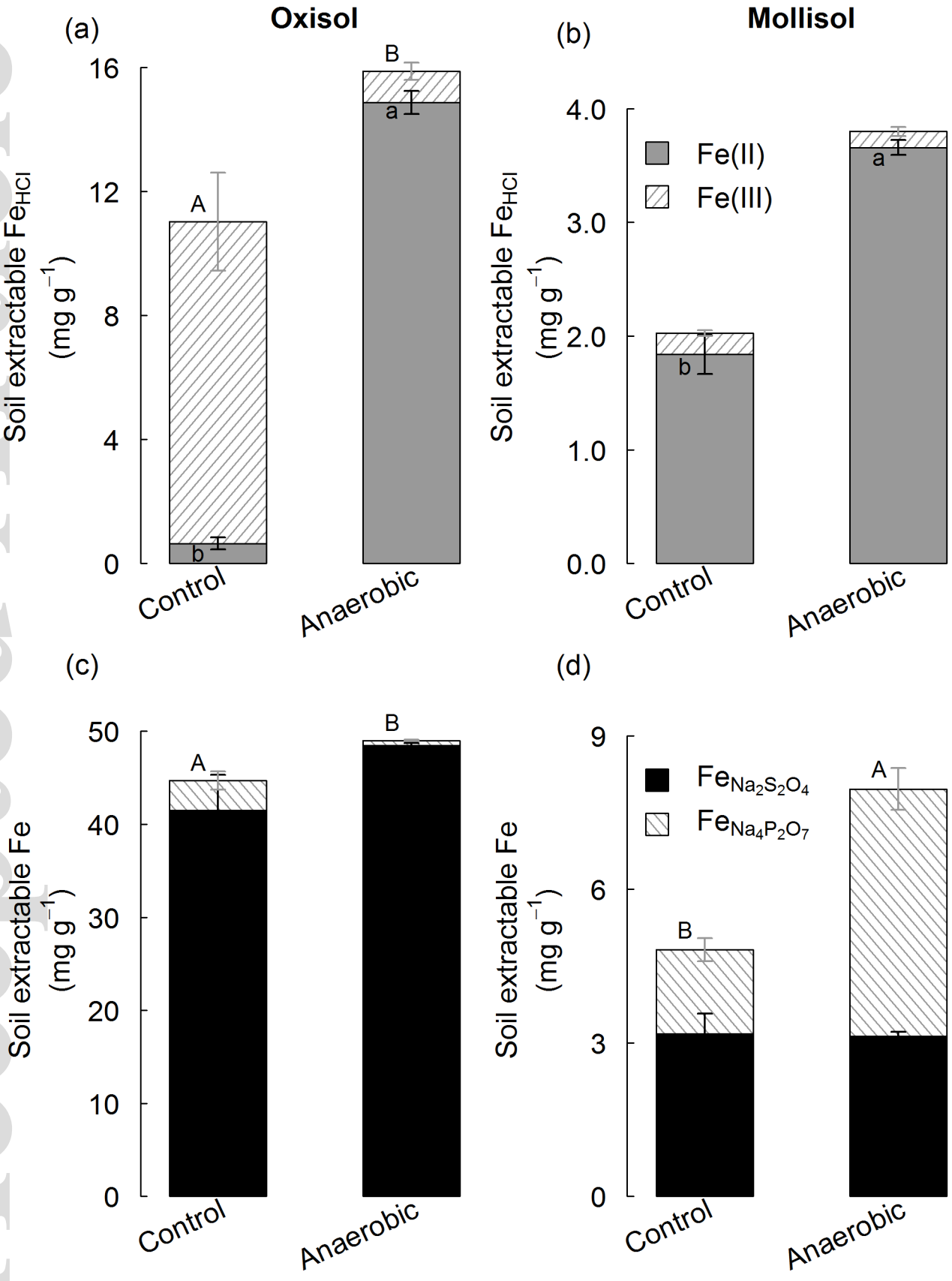

gcb_15100_f2.png

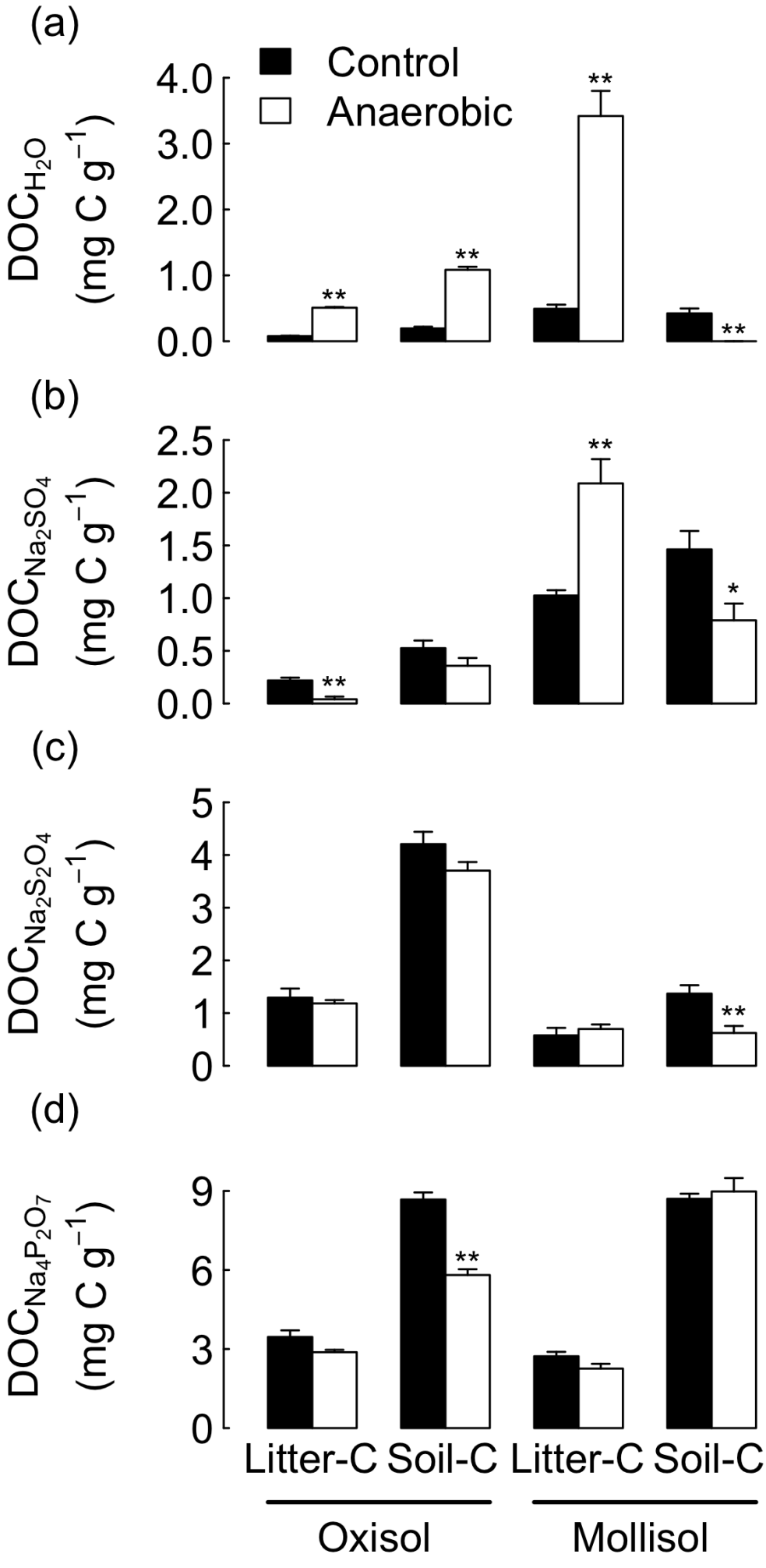

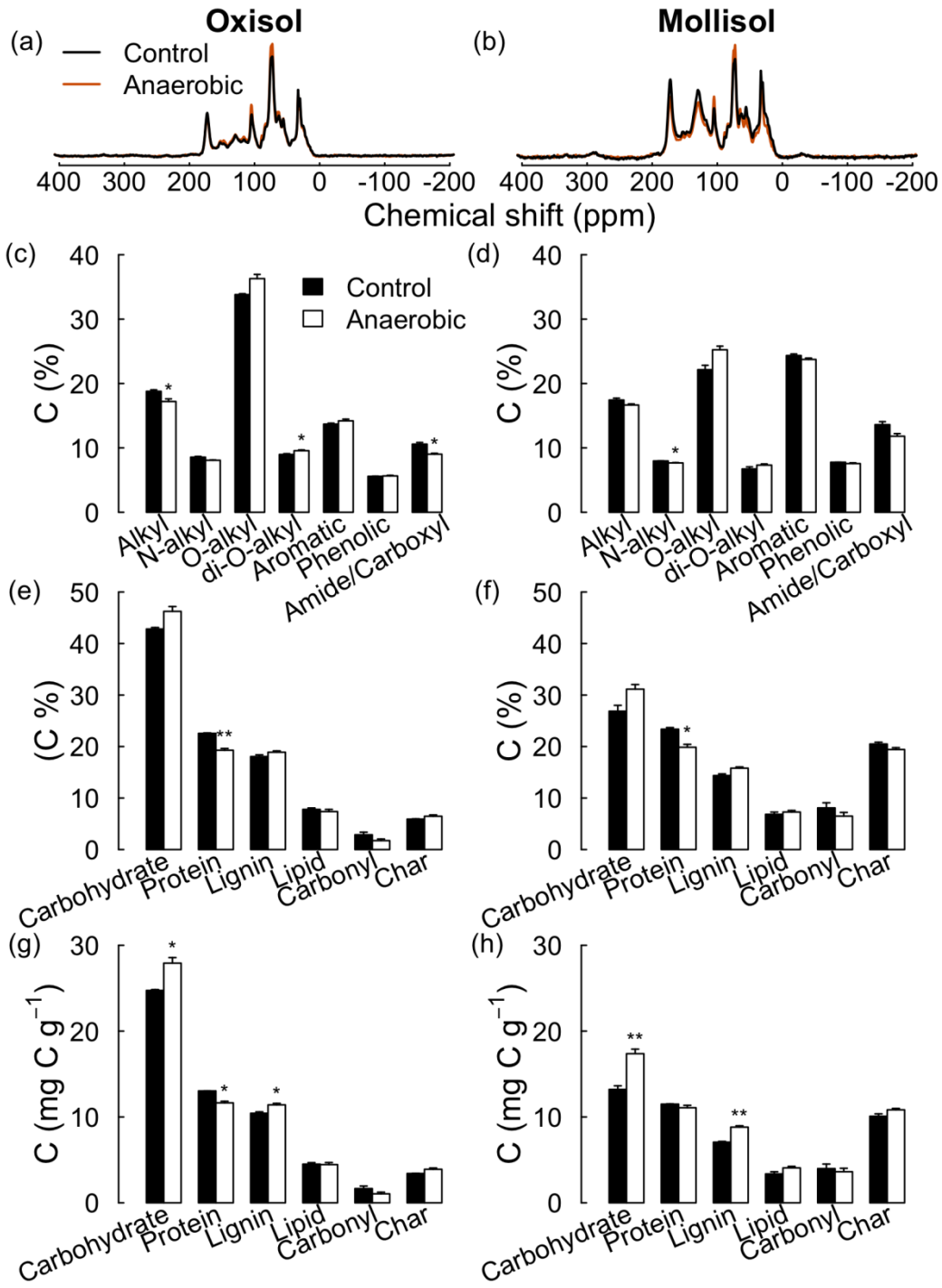

gcb_15100_f4.png